Supporting Information for:

Supramolecular Fibers In Gels Can Be At Thermodynamic Equilibrium: A Simple Packing Model Reveals Preferential Fibril Formation *Versus* Crystallization

Ivan Ramos Sasselli,[†] Peter J. Halling,[†] Rein V. Ulijn,*[,†,‡] and Tell Tuttle*[,†]

[†] Pure and Applied Chemistry Department, WestCHEM, University of Strathclyde, 295 Cathedral Street, Glasgow, G1 1XL, UK.

[‡]Advanced Science Research Center and Hunter College, City University of New York, 85 St Nicholas Terrace, New York, NY 10031, USA.

KEYWORDS Low molecular weight gelators, amphiphiles, soft-matter, gel, self-assembly, thermodynamics, packing, model

Sq Formulation:

Table S1. Expressions for the calculation of the fiber Gibbs energy (G_{fiber}) for *Sq* with the different values of *n*.

Sq_0	$G_{fiber} = (2f_2 + f_1) \cdot \gamma_{ks} + (4f_2 + 5f_1 + 6f_0) \cdot \gamma_{kb}$
Sq_1	$G_{fiber} = (f_2 + f_1) \cdot \gamma_{ls} + f_0 \cdot \gamma_{lb} + f_2 \cdot \gamma_{ks} + (4f_2 + 5f_1 + 5f_0) \cdot \gamma_{kb}$
Sq_2	$G_{fiber} = (2f_2 + f_1) \cdot \gamma_{ls} + (f_1 + 2f_0) \cdot \gamma_{lb} + (4f_2 + 4f_1 + 4f_0) \cdot \gamma_{kb}$
Sq_3	$G_{fiber} = (2f_2 + f_1) \cdot \gamma_{ls} + (f_2 + 2f_1 + 3f_0) \cdot \gamma_{lb} + (3f_2 + 3f_1 + 3f_0) \cdot \gamma_{kb}$

Table S2. Expressions and minimum values for the crystal Gibbs energy (G_{crys}) and solvation excess Gibbs energies (G_{solv}) for *Sq* with the different values of *n*.

	G_{crys}	G_{solv}	$G_{crys,min}$	$G_{solv,min}$
Sq_0	$6 \cdot \gamma_{kb}$	$6 \cdot \gamma_{ks}$	6	12
Sq_1	$\gamma_{lb} + 5 \cdot \gamma_{kb}$	$\gamma_{ls} + 5 \cdot \gamma_{ks}$	5	10
Sq_2	$2 \cdot \gamma_{lb} + 4 \cdot \gamma_{kb}$	$2 \cdot \gamma_{ls} + 4 \cdot \gamma_{ks}$	4	8
Sq_3	$3 \cdot \gamma_{lb} + 3 \cdot \gamma_{kb}$	$3 \cdot \gamma_{ls} + 3 \cdot \gamma_{ks}$	3	6

Regular Shapes:

Squares based prims may not always be the best way of representing LMWGs but the theory can be extended to other prisms: with triangular (*Tr*) and with hexagonal (*Hx*) base. These are with *Sq* the simplest prism with perfect packing in the cross sections. All the faces are considered to have the same area. The formulation was derived as described for *Sq*. *Hx* show a main difference with the other two units, their fiber faces units expose 2 faces to the solvent ($m=2$) and the corner units 3 ($m_{max}=3$), while for *Sq* and *Tr* they are 1 and 2 respectively (Fig. S1).

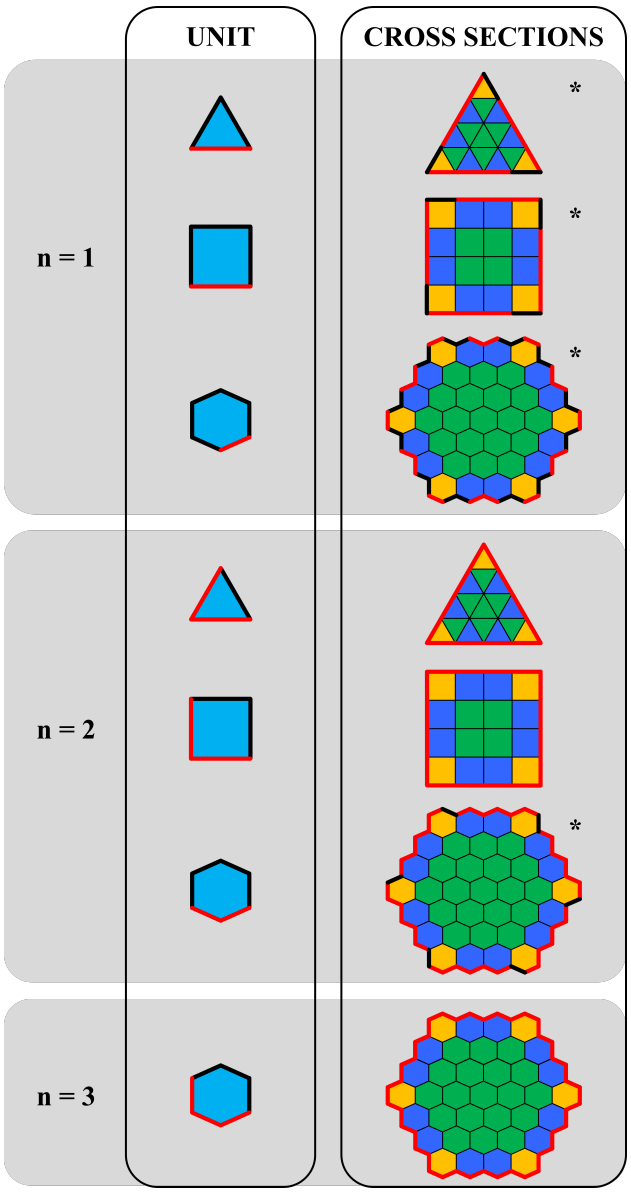

Figure S1. Cross sections of the three shapes with *n=1* and *n=2* for the three and with *n=3* for the hexagons. It shows solvophilic faces (red) and solvophobic faces (black) exposed to the solvent. The cross sections show buried units in green, units on the fiber faces in blue and units in the fiber corners in yellow (m_{max}). *Cross sections which propitiate fibers exposing both solvophilic and –phobic faces to the solvent.

The f_m changes with d differ for the different shapes (Fig. S2). All have in common the fast decrement of f_{max} and that the three components are important at low d´s. *Sq* is the only unit which has only corner units at $d=0$ and the fraction of core units increases the

fastest for *Hx*. The formulation for different shapes gives different possibilities to fit the model to real LMWG.

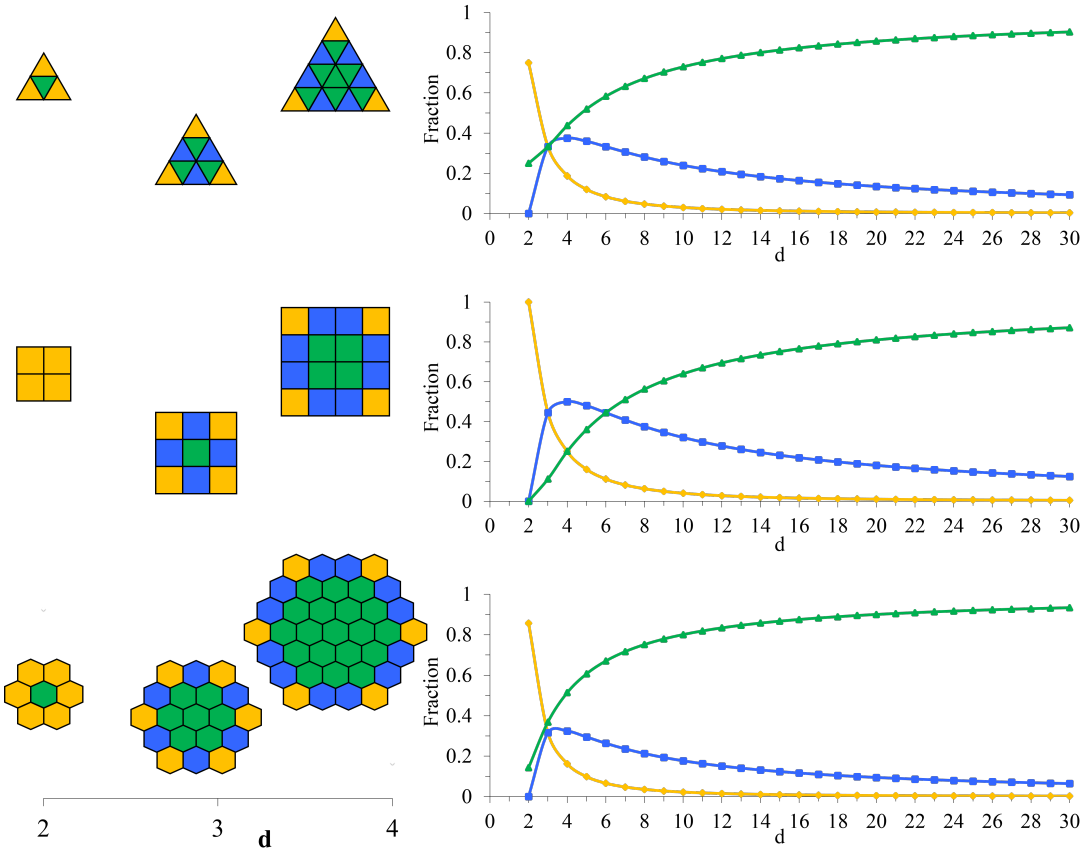

Figure S2. Evolution of the fractions of units which can be buried (green), on the faces of the fiber (blue) and on the corners of the fiber (yellow) as a function of *d*, for the different units. Examples for d=2-4 (left) and graphic for d=2-30 (right).

The fractions equations for the three shapes are presented in Table S3 and the equations for the G_{fiber} of the different units with the different *n´s* are presented in Table S4.

Table S3. Fractions of units (f_m) with *m* faces exposed to the solvent for the different regular shapes.

	Triangle (Tr)	Square (Sq)	Hexagon (Hx)
Buried	$f_0 = \frac{d^2 - 3d + 3}{d^2}$	$f_0 = \frac{(d-2)^2}{d^2}$	$f_0 = \frac{3d^2 - 9d + 7}{3d^2 - 3d + 1}$
Fiber side	$f_1 = \frac{3(d-2)}{d^2}$	$f_1 = \frac{4(d-2)}{d^2}$	$f_2 = \frac{6(d-2)}{3d^2 - 3d + 1}$
Fiber corner	$f_2 = \frac{3}{d^2}$	$f_2 = \frac{4}{d^2}$	$f_3 = \frac{6}{3d^2 - 3d + 1}$

Table S4. Expressions for the calculation of the fiber Gibbs energy (G_{fiber}) for the different regular shapes.

Tr_1	$G_{fiber} = (f_2 + f_1) \cdot \gamma_{ls} + f_0 \cdot \gamma_{lb} + f_2 \cdot \gamma_{ks} + (3f_2 + 4f_1 + 4f_0) \cdot \gamma_{kb}$
Sq_1	$G_{fiber} = (f_2 + f_1) \cdot \gamma_{ls} + f_0 \cdot \gamma_{lb} + f_2 \cdot \gamma_{ks} + (4f_2 + 5f_1 + 5f_0) \cdot \gamma_{kb}$
Hx_1	$G_{fiber} = (f_3 + f_2) \cdot \gamma_{ls} + f_0 \cdot \gamma_{lb} + (2f_3 + f_2) \cdot \gamma_{ks} + (5f_3 + 6f_2 + 7f_0) \cdot \gamma_{kb}$
Tr_2	$G_{fiber} = (2f_2 + f_1) \cdot \gamma_{ls} + (f_1 + 2f_0) \cdot \gamma_{lb} + (3f_2 + 3f_1 + 3f_0) \cdot \gamma_{kb}$
Sq_2	$G_{fiber} = (2f_2 + f_1) \cdot \gamma_{ls} + (f_1 + 2f_0) \cdot \gamma_{lb} + (4f_2 + 4f_1 + 4f_0) \cdot \gamma_{kb}$
Hx_2	$G_{fiber} = (2f_3 + 2f_2) \cdot \gamma_{ls} + 2f_0 \cdot \gamma_{lb} + f_3 \cdot \gamma_{ks} + (5f_3 + 6f_2 + 6f_0) \cdot \gamma_{kb}$
Hx_3	$G_{fiber} = (3f_3 + 2f_2) \cdot \gamma_{ls} + (f_2 + 3f_0) \cdot \gamma_{lb} + (5f_3 + 5f_2 + 5f_0) \cdot \gamma_{kb}$

Table S5. Expressions and minimum values for the crystal Gibbs energies (G_{crys}) and solvation excess Gibbs energies (G_{solv}) for the different regular shapes.

	G_{crys}	G_{solv}	$G_{crys,min}$	$G_{solv,min}$
Tr_1	$\gamma_{lb} + 4 \cdot \gamma_{kb}$	$\gamma_{ls} + 4 \cdot \gamma_{ks}$	4	8
Sq_1	$\gamma_{lb} + 5 \cdot \gamma_{kb}$	$\gamma_{ls} + 5 \cdot \gamma_{ks}$	5	10
Hx_1	$\gamma_{lb} + 7 \cdot \gamma_{kb}$	$\gamma_{ls} + 7 \cdot \gamma_{ks}$	7	14
Tr_2	$2 \cdot \gamma_{lb} + 3 \cdot \gamma_{kb}$	$2 \cdot \gamma_{ls} + 3 \cdot \gamma_{ks}$	3	6
Sq_2	$2 \cdot \gamma_{lb} + 4 \cdot \gamma_{kb}$	$2 \cdot \gamma_{ls} + 4 \cdot \gamma_{ks}$	4	8
Hx_2	$2 \cdot \gamma_{lb} + 6 \cdot \gamma_{kb}$	$2 \cdot \gamma_{ls} + 6 \cdot \gamma_{ks}$	6	12
Hx_3	$3 \cdot \gamma_{lb} + 5 \cdot \gamma_{kb}$	$3 \cdot \gamma_{ls} + 5 \cdot \gamma_{ks}$	5	10

The results are separated in amphiphilic ($n<m_{max}$) and non-amphiphilic ($n=m_{max}$) fibers. The ΔG_{fiber} plots as a function of γ_{ks} for amphiphilic fibers (Fig. S3) use a fixed value of γ_{lb} (=2). They show a similar profile for Tr_1 and Sq_1 (Fig. S3 A and B). Both shapes (n=1) present values of ΔG_{fiber} lower than 0 and with d_{min} lower than 10 for a wide range of γ_{ks}. The global minimum in the surface appears at the minimum value of γ_{ks}, which involves the minimum possible destabilization that results from exposing a solvophobic face to solvent. It corresponds with the minimum value of d_{min} and hence the thinnest fiber ($d=3$). As γ_{ks} increases the thermodynamically favored fiber is wider because that reduces the fraction of solvophobic faces exposed to the solvent (f_2, Fig. S2). But even after increasing it by a factor of 4, the fiber width is only 3 times greater.

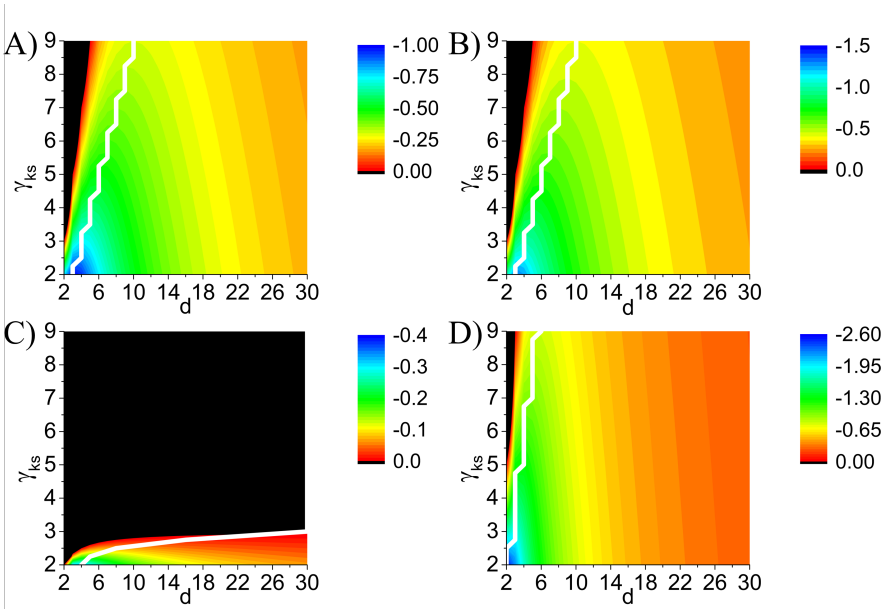

Figure S3. ΔG_{fiber} as a function of d and γ_{ks} with fixed γ_{lb} for amphiphilic fibers: Tr_1 (A), Sq_1 (B), Hx_1 (C) and Hx_2 (D). d_{min} is represented with a white line.

The plot for the Hx_1 clearly differs from the rest (Fig. S3 C). This plot shows that d_{min} rises faster when increasing the value of γ_{ks} than for the other cases. Even for values of γ_{ks} only slightly greater than 3, d_{min} is already higher than 30, which suggest that the fiber is not the thermodynamic favored product on this case. This is not surprising because for this shape more than the half of the faces exposed to solvent are solvophobic. This can only be stable when the loss of stabilization due to this exposure is very low, as shown in the graph. Nevertheless, when the *Hx* unit has two solvophilic faces (Hx_2), it reduces the number of solvophobic faces exposed to the solvent to almost the half and the plot shows a profile more similar to the Tr_1 and Sq_1 (Fig. S3 A and B). It actually tends to form thinner fibers than these, due to the fact that N increases faster with d for the *Hx* and hence the number of core units with solvophilic faces buried as well (Fig. S2).

The ΔG_{fiber} plots as a function of γ_{lb} (Fig. S4) take into account that $G_{crys}<G_{solv}$, and hence, the fixed value for G_{solv} is the highest G_{crys} in the plot range plus 1. The value of γ_{ks} is then calculated: 3.5 (Tr_1), 3 (Sq_1), 2.4 (Hx_1) and 3.8 (Hx_2).

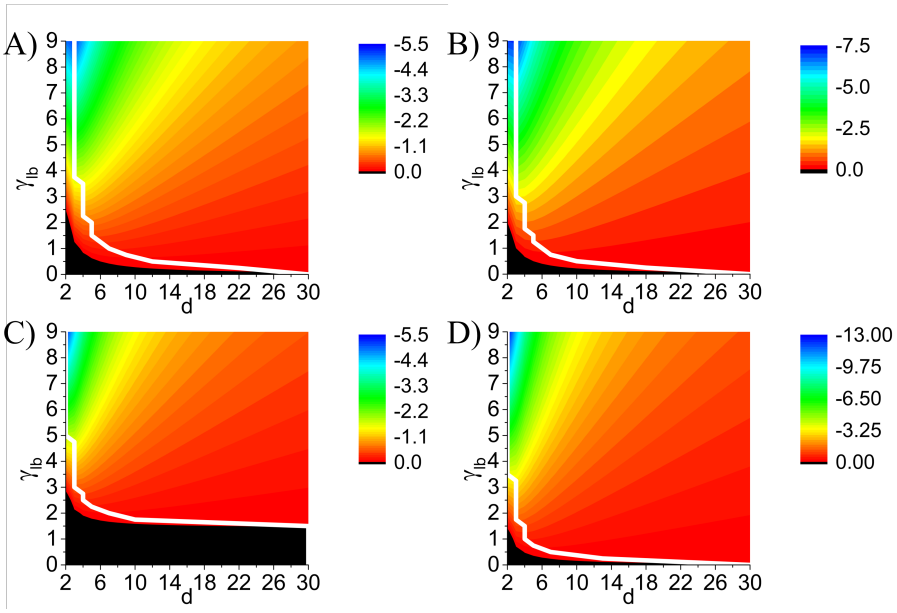

Figure S4. ΔG_{fiber} as a function of d and γ_{lb} with fixed γ_{ks} for amphiphilic fibers: Tr_1 (A), Sq_1 (B), Hx_1 (C) and Hx_2 (D). d_{min} is represented with a white line.

The ΔG_{fiber} plots show similar profiles for the four cases (Fig. S4). All show a minimum with ΔG_{fiber} lower than 0. This is a shallow minimum for low values of γ_{lb} which becomes deeper as the parameter increases. d_{min} also decreases as this parameter rises. These tendencies are due to the increasing destabilization of the buried solvophilic faces with the parameter γ_{lb}, which also enhances the destabilizing effect of increasing d.

In general, the minimum d_{min} correspond to the minimum difference between G_{crys} and G_{solv}. This is consistent with the experimental observations which shows that molecules with a limited solubility have a higher tendency to form fibers. Bigger fibers are expected as this difference gets higher ($G_{crys} << G_{solv}$).

For non-amphiphilic fibers (Tr_2, Sq_2 and Hx_3) the trends in the plots are different to the previous (Fig. S5). First of all, as there is no solvophobic face exposed to the solvent there is no dependence with the parameter γ_{ks} and therefore the plots with the fixed γ_{lb} are only shown as a function of d (Fig. S5 D). All the plots show negative ΔG_{fiber} supporting the idea that also non-amphiphilic fibers can also be at thermodynamic equilibrium. Furthermore, the d_{min} adopts the minimum possible value in all the cases (d=2) because the only destabilizing effect corresponds to burying solvophilic faces, the number of which increases with d.

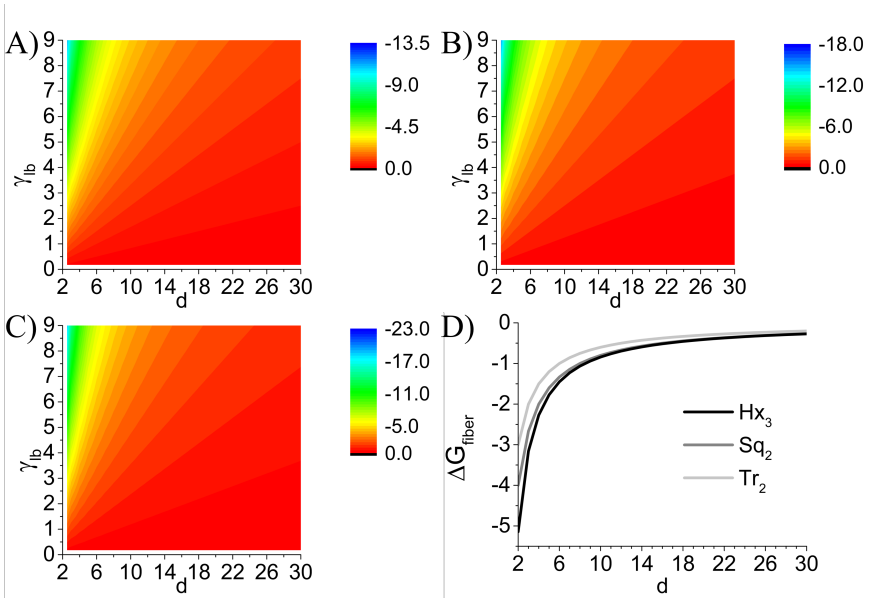

Figure S5. ΔG_{fiber} for non-amphiphilic fibers as a function of d and: γ_{lb} with fixed γ_{ks} Tr_2 (A), Sq_2 (B), Hx_3 (C) and with fixed γ_{lb} for Tr_2, Sq_2 and Hx_3 (D). d_{min} is represented with a white line in graphs A-C.

The fact that similar results are obtained even changing the shape of the units confirms the validity of the model and gives more possibilities to mimic real systems.

Irregular Shapes: 3D Cross Section for *Hx*.

Experimentally there are other types of nanostructures besides fibers, like the 2D objects, tapes and sheets. These nanostructures can still be assumed to grow infinitely in the z-direction but they also considerably grow in one direction of the xy-plane. *Hx* were reformulated in function of three dimensions (d_x, d_y and d_z) in the xy-plane (Fig. S6) using Hx_2 and Hx_3 as units because they showed good results in the one-dimensional formulation.

Table S6. Fractions of units (f_m) with *m* faces exposed to the solvent for the *Hx* as a function of d_x, d_y and d_z.

	Hexagon (Hx)
Buried	$f_0 = \frac{(d_xd_y + d_xd_z + d_yd_z) - 3(d_x + d_y + d_z) + 7}{(d_xd_y + d_xd_z + d_yd_z) - (d_x + d_y + d_z) + 1}$
Fiber side	$f_2 = \frac{2(d_x + d_y + d_z - 6)}{(d_xd_y + d_xd_z + d_yd_z) - (d_x + d_y + d_z) + 1}$
Fiber corner	$f_3 = \frac{6}{(d_xd_y + d_xd_z + d_yd_z) - (d_x + d_y + d_z) + 1}$

Figure S6. Evolution of the fractions of units which can be buried (green), on the faces of the fiber (blue) and on the corners of the fiber (yellow) as a function of three directions (d_x, d_y and d_z) on the cross section plane (xy-plane).

The ΔG_{fiber} are shown as a function of two of the dimensions in the xy-plane: d_x and d_y. As the three directions are equivalent to each other, this is enough to see if the system tends to grow or not in just one of these dimensions. It can be seen that for non-amphiphilic fibers, Hx_3, the system shows the minimum excess Gibbs energy for small *d's* with no difference between them (Fig. S7 D-F), suggesting fibers to be the thermodynamic favored product for these systems independently to the different interaction parameters tried. However, the amphiphilic fibers show different behaviors with different interaction parameters (Fig. S7 A-C). The case where the excess energy of burying a solvophilic face is more favorable than exposing a solvophobic face ($\gamma_{lb}<\gamma_{ks}$) the structure clearly shows

(Fig. S7 A) a preference for a 2D growth ($G_{fiber,min}$ corresponds to $d_x=30$ and $d_y=2$). For the other two cases the preference is not that clear and the G_{fiber} is relatively shallow. For the case where both parameters have the same value ($\gamma_{lb}=\gamma_{ks}$) the actual $\Delta G_{fiber,\,min}$ (Fig. S7 B) corresponds also to a 2D structure ($d_x=30$ and $d_y=2$) while when the energy penalty of burying solvophilic faces is greater ($\gamma_{lb}>\gamma_{ks}$) the fibers ($d_x=d_y=2$) are the preferred product (Fig. S7 C).

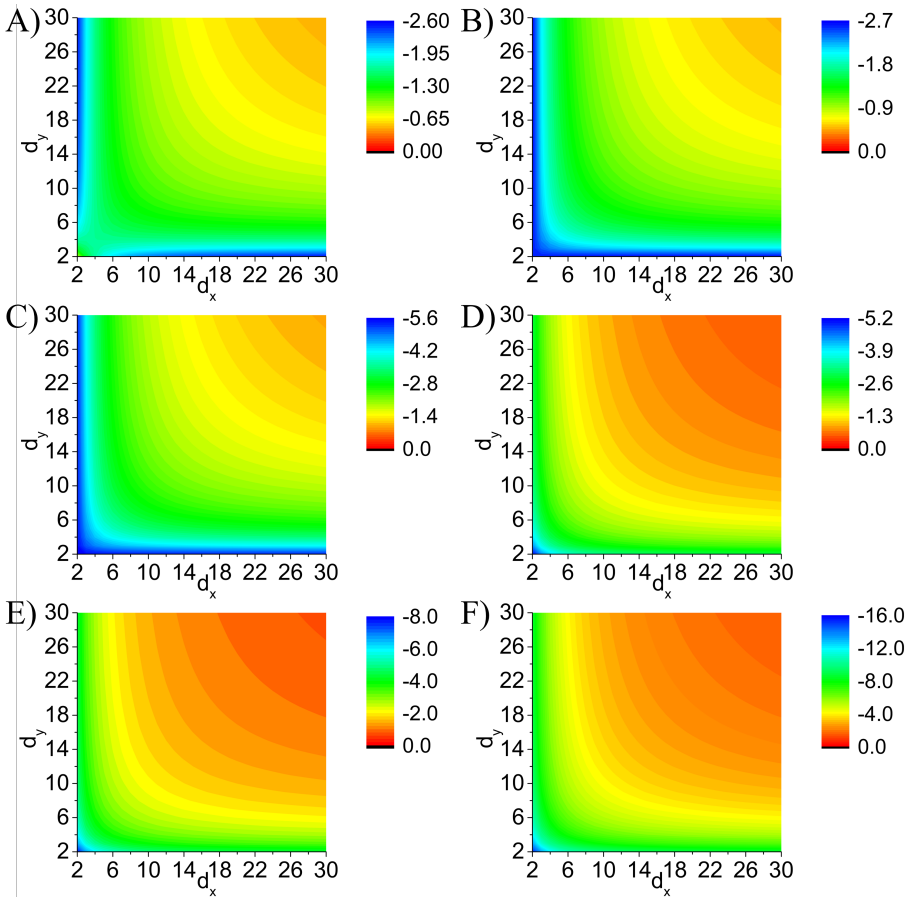

Figure S7. ΔG_{fiber} as a function of d_x and d_y for Hx_2 (A-C) and Hx_3 (D-F) with fixed values of γ_{lb} and γ_{ks}: 2:4 (A), 2:2 (B), 4:2.5 (C), 2:4 (D), 3:3 (E) and 6:5 (F).

Application to Real LMWG.

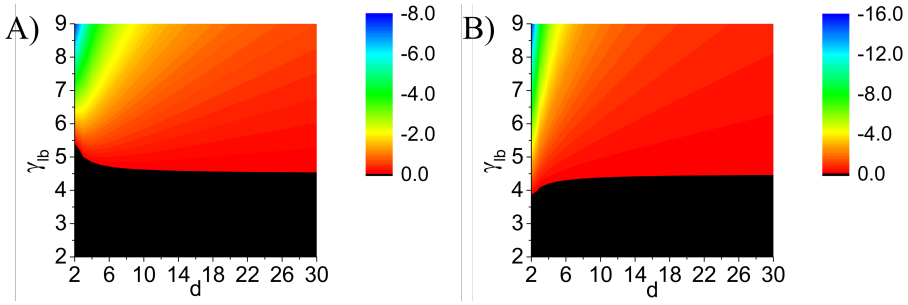

Figure S8. ΔG_{fiber} as a function of *d* and as a function of γ_{lb} for Hx_1 (A) and Hx_{1+1} (B). The rest of the parameters change as indicated in Fig. 3 E.